Electrode effect on high-detectivity ultraviolet photodetectors based on perovskite oxides

Wen-jia Zhou, Kui-juan Jin, Hai-zhong Guo, Chen Ge, Meng He et al.

Citation: J. Appl. Phys. **114**, 224503 (2013); doi: 10.1063/1.4845775
View online: http://dx.doi.org/10.1063/1.4845775
View Table of Contents: http://jap.aip.org/resource/1/JAPIAU/v114/i22
Published by the AIP Publishing LLC.

Additional information on J. Appl. Phys.

Journal Homepage: http://jap.aip.org/
Journal Information: http://jap.aip.org/about/about_the_journal
Top downloads: http://jap.aip.org/features/most_downloaded
Information for Authors: http://jap.aip.org/authors

Electrode effect on high-detectivity ultraviolet photodetectors based on perovskite oxides

Wen-jia Zhou, Kui-juan Jin,[a] Hai-zhong Guo, Chen Ge, Meng He, and Hui-bin Lu
Institute of Physics, Beijing National Laboratory for Condensed Matter Physics, Chinese Academy of Sciences, Beijing 100190, People's Republic of China

(Received 10 September 2013; accepted 25 November 2013; published online 10 December 2013)

High-detectivity metal-semiconductor-metal ultraviolet photodetectors have been fabricated based on $SrTiO_3$ with different types of metal electrodes (Ag, Ni, and Pt), and the effects of the different types of the electrodes on the photoelectric properties were investigated. Comparing with three types of the metal electrodes, the largest responsivity of 0.517 A/W and the smallest dark current of 2.215×10^{-11} A were obtained by using Ag electrode due to the largest Schottky barrier between Ag electrode and $SrTiO_3$. The detectivities of all the photodetectors are achieved about 10^{12} cm·HZ$^{1/2}$/W, which can be comparable to Si-based photodetectors. Furthermore, a transient photovoltaic signal with a rise time of ~360 ps and a full width at half-maximum of ~576 ps are obtained in the Ag/$SrTiO_3$/Ag photodetectors under the illumination of a 355 nm laser with 15 ps duration. These results provide a useful guide for designing high-performance photodetectors based on perovskite oxides and the appropriate metal electrode selected. © *2013 AIP Publishing LLC*. [http://dx.doi.org/10.1063/1.4845775]

I. INTRODUCTION

Visible-blind ultraviolet (UV) photodetectors have drawn a great deal of interest for their applications in variety of industrial, military, and scientific fields, including communications, automotive, flame detection, biological research, chemical sensing, and image sensing.[1–4] Conventional semiconductor like Si and gallium arsenide can be used to UV detection, but filters are needed to exclude their long wavelength response.[5] Wide band gap materials including ZnO, GaN, and SiC are attractive candidates for UV photodetectors.[6–8] Perovskite oxides with wide band gap, which have strong stability against high temperature and strong radiation, have potential to be new candidates for next-generation UV photodetectors, also due to their multi-coupling property and the multi-freedom manipulating.[9,10] We have successfully fabricated different types of UV photodetectors based on perovskite oxides such as $SrTiO_3$ (STO),[11,12] $LaAlO_3$,[13] $LiTaO_3$,[14] and $LiNbO_3$.[15] We have also reported paralleled detector cells based on STO to increase the photocurrent.[16] For fabricating photodetectors and other devices, the selection of electrode material is an important issue due to the variation of the work functions of metals and different types of the contacting, as well. Taking STO as an example, both Ohmic and Schottky contacts were observed depending on different electrode materials.[17–19] Electrode-dependent transport properties of metal/STO and metal/doped-STO structures were investigated and thought to be influenced by the Schottky effect and interface states.[19,20] Schottky barrier height between a series of metals and STO has also been calculated using the first-principles and other methods.[18,21,22] In this work, by using different types of metals as electrodes, three kinds of metal-semiconductor-metal (MSM) ultraviolet photodetectors based on STO single crystals have been fabricated and their performances have been investigated. The differences of the photoresponse with different metal electrodes are obvious. All of the photodetectors have low dark current and high normalized detectivity (D*), which can be comparable to Si-based photodetectors.

II. EXPERIMENT

The UV Photodetectors of MSM structure were fabricated based on single polished STO single-crystal wafers with a size of $10 \times 10 \times 0.5$ mm^3 by using standard optical photolithography and lift-off technique. In order to investigate the influence of different metal contacts on the performance, we have fabricated three kinds of detectors using different metal electrodes with different values of work function. Ag (50 nm) and Ni (5 nm)/Au (50 nm) were deposited by thermal evaporation, while Pt (50 nm) was deposited by pulsed laser deposition method. Figure 1(a) shows the optical micrograph of the STO-based Photodetectors. The interdigital electrodes are 320 μm long and 10 μm wide, and have an inter-electrode spacing of 10 μm. The total sensing area of the detector is 320×510 μm^2. The structures and dimensions of these three kinds of the detectors are all the same. The current-voltage (I-V) characteristics of these three devices were measured by using Keithly 6517B and Keithly 2400 source meter units. The spectra response was performed by using a monochromator combined with a 30 W Xe lamp, an optical chopper and a lock-in amplifier.

III. RESULTS AND DISCUSSIONS

Figure 1(b) shows the I-V curves of these three kinds of devices in dark at room temperature. The electrode arrangement is illustrated schematically in the inset of Figure 1(b). From Figure 1(b), it can be observed that these three devices show a typical MSM type I-V characteristics, and the dark

[a]Author to whom correspondence should be addressed. Electronic mail: kjjin@iphy.ac.cn

 © 2013 AIP Publishing LLC

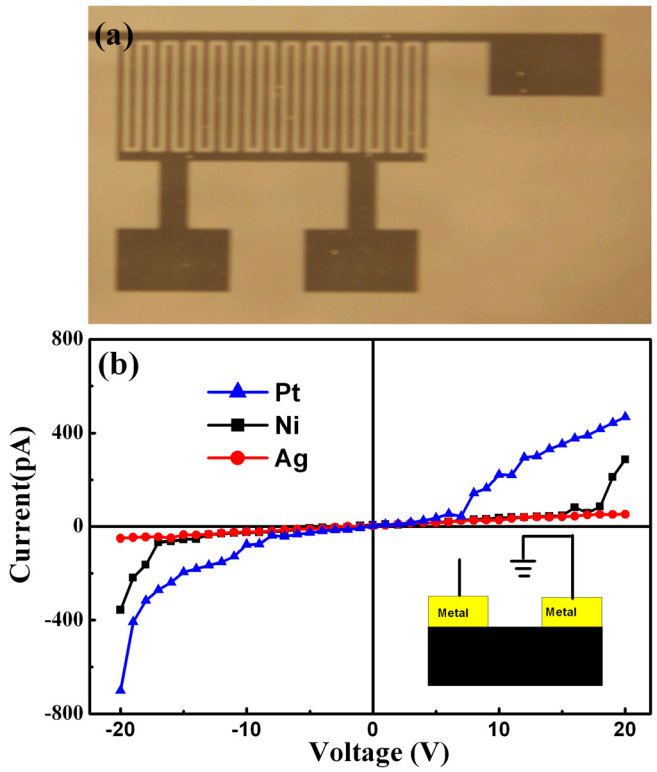

FIG. 1. (a) The optical photograph of interdigitated electrodes. (b) *I-V* characteristics of the three kinds of the detectors in dark. The structure diagram is shown in the inset.

currents of the Ag/STO/Ag, Ni(Au)/STO/Ni(Au), and Pt/STO/Pt devices under 10 V bias are 2.215×10^{-11}, 2.69×10^{-11}, and 3.56×10^{-11} A, respectively. The low dark current is helpful to enhance the signal-to-noise(S/N) ratio of the photodetector. As we all know, the work functions of Ag, Ni, and Pt are about 4.2, 5.1, and 5.6 eV, respectively. Therefore, the dark current increases with the increase of the work function of the electrode materials. To obtain further insight of the intrinsic physics, the energy diagram of the MSM structure is illustrated in Figure 2(a). The electron affinity of STO is about 4.1 eV and the band gap is 3.2 eV.[19,21,23] For intrinsic semiconductor, Fermi Level is located in the middle of the band gap, therefore the work function of STO here is taken as about 5.7 eV. Normally undoped titanate crystals and ceramics are usually governed by an unknown concentration of acceptor-type impurities.[19,24,25] Therefore, the STO crystals, in this study, were taken as slightly acceptor-doped materials. In the case of acceptor-type semiconductors, the barrier heights of the contact of semiconductors with low work function metals are larger than those high work function metals. For these three types of metal-STO Schottky contact, Ag/STO has the largest Schottky barrier, while Pt/STO has the lowest Schottky barrier, which are shown in Figure 2(a). We assume that thermionic emission of electrons surmount the metal/STO Schottky barriers to determine the current flow. For the Ag/STO/Ag structure, carriers need to overcome a larger barrier to contribute to the current flow, therefore the detector with this structure has the lowest dark current, while the detector with Pt/STO/Pt structure has the largest dark current.

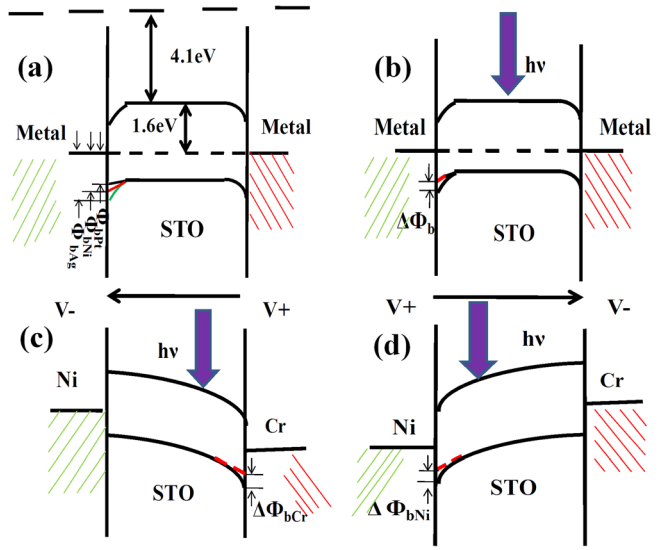

FIG. 2. (a) Band diagram of the metal/STO/metal photodetectors. ϕ_{bAg}, ϕ_{bNi}, and ϕ_{bPt} stand for the Schottky barriers of the STO and different electrodes, respectively. (b) The reduction of the schottky barrier $\Delta\phi_b$ under ultraviolet light illumination. (c) Band diagram of the Ni/STO/Cr photodetector under illumination when positive bias applied on the Cr side. (d) Band diagram of the Ni/STO/Cr photodetector under illumination when negative bias applied on the Cr side.

The optical transmittance spectra of STO crystal were shown in Figure 3(a) and the spectral responses of the three kinds of detectors at 10 V bias were shown in Figure 3(b). Within the visible region, the average transmittance of the STO wafer is over 70%. It exhibits a sharp absorption edge at 390 nm, which is consistent with the band gap of 3.2 eV.

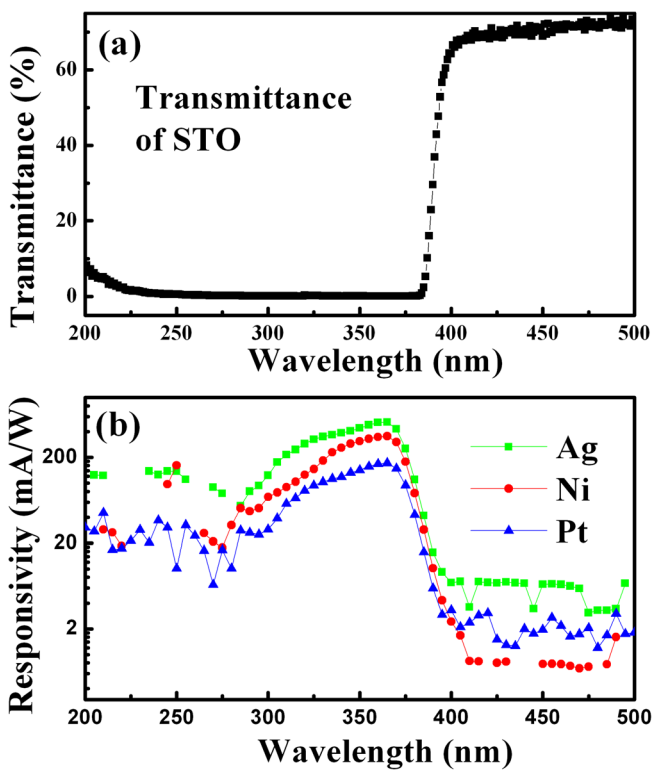

FIG. 3. (a) Transmission spectra of the STO single crystal. (b) Spectral response of Ag/STO/Ag, Ni(Au)/STO/Ni(Au), and Pt/STO/Pt detectors at 10 V bias.

As shown in Figure 3(b), the spectral responses of these three kinds of photodetectors also show the same response edges as 390 nm, which is in agreement with the transmission spectral results. For all the MSM photodetectors with different types of metal electrodes, the wavelengths of the peak responsivity were all at 365 nm. The maximum responsivities of MSM photodetectors with Ag, Ni, and Pt electrodes illuminated under 365 nm at 10 V bias are 0.517, 0.353, and 0.171 A/W, respectively. Comparing with STO-based photodetectors reported before,[10] larger responsivity was obtained in these MSM photodetectors because of the different electrodes we used. The degree of "visible blindness", i.e., the ultraviolet/visible rejection ratio, we defined as the ratio between the values of responsivity R at 365 nm and 400 nm, is about two orders of magnitude, indicating a high degree of visible blindness. Among the three kinds of photodetectors, it can be found that the maximum responsivity increases with the decrease of the work function of metal electrode. Previously, we have showed that the Ag/STO/Ag structure had the lowest dark current, it is interesting that it also has the largest responsivity.

In order to explain the origin of the electrode-dependent photoelectric properties of the MSM photodetectors, the band diagram of the MSM structure under illumination was shown in Figure 2(b). When ultraviolet light illuminates the photodetector, the Schottky barrier will be lowered. The reduction of Schottky barrier is $\Delta\Phi_b$. It is reported that there is a relationship between the responsivity and $\Delta\Phi_b$[26]

$$R = \frac{\exp\left(\frac{\Delta\phi_b}{KT}\right) I_{dark} - I_\lambda}{W}, \tag{1}$$

where R is the responsivity of the detector, $\Delta\Phi_b$ is the reduction of Schottky under certain condition like illumination, I_{dark} is the dark current, I_λ is the primary current, and W is the light intensity. The reduction of Schottky barrier under illumination would enhance the photoresponse. Considering the result that the electrode with lower work function has a larger responsivity, it is inferred that the electrode with lower work function has a larger $\Delta\Phi_b$ under illumination. In order to prove this point, we fabricated a detector with asymmetric electrodes of Ni/STO/Cr structure (the distance between the electrodes is 50 μm). Figure 4 shows the dark current and photocurrent of the detector under the illumination of a Xe lamp. The polarity of the applied bias is defined as positive when applied to the Cr/STO Schottky contact. The measurement began at -30 V applying to the Cr/STO Schottky contact. The MSM structure can be modeled as being composed of two Schottky barriers "head to head" in series. When a voltage was supplied, there is always a Schottky barrier, which is in positive bias, while the other is in reverse bias. The current of the structure is dominated by the barrier in reverse bias. As shown in Figure 2(c), in the positive region, the Cr/STO barrier is in reverse bias and the current of the structure is dominated by the Cr/STO barrier. In contrast, in the negative region as shown in Figure 2(d), the Ni/STO barrier was in reverse bias and dominated the current of the detector. It can be seen from Figure 4 that the variation

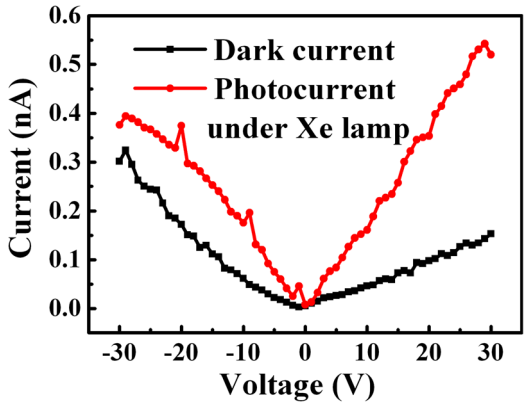

FIG. 4. Dark current and photo current under illumination of Xe light of the Ni/STO/Cr photodetector.

between the photocurrent and the dark current in the positive region is larger than that in the negative region. This indicates that under illumination the reduction of Cr/STO Schottky barrier $\Delta\Phi_{bCr}$ is larger than that of Ni/STO Schottky barrier $\Delta\Phi_{bNi}$. The work functions of Cr and Ni are 4.5 and 5.1 eV, respectively. Thus, this result supports our point that the electrode with lower work function has a larger $\Delta\Phi_b$ under illumination. Therefore, the Ag/STO/Ag structure has the largest responsivity and the responsivity increases with the decrease of the work function of metal electrode can be explained.

The noise equivalent power (NEP) and D* are two important figures of merit of the photodetector. There are three contributions to the noise that limits D^*: shot noise from dark current, Johnson noise, and thermal fluctuation "flicker" noise.[3] Here, the thermally limited mode may not be applied as the shot noise is significant. Therefore, the NEP can be calculated by

$$NEP = \left(\frac{4k_bT}{R_{dark}} + 2qI_{dark}\right)^{1/2} \Big/ R_\lambda, \tag{2}$$

where R_{dark} refers to the device differential resistance, I_{dark} is the dark current, and R_λ is the responsivity at the selected optical wavelength (λ).[27–29] Then, D^* can be determined by

$$D^* = \sqrt{A}/NEP, \tag{3}$$

where A is the active area of the device. With a 10 V applied bias at 365 nm, the corresponding NEP of the Ag/STO/Ag, Ni(Au)/STO/Ni(Au), and Pt/STO/Pt device are 7.09×10^{-15}, 7.50×10^{-15}, and 2.28×10^{-14} W/HZ$^{1/2}$, respectively. D^* of the three detectors are 4.11×10^{12}, 3.88×10^{12}, and 1.27×10^{12} cm·HZ$^{1/2}$/W, respectively. In the UV region, the D^* of Si-based detectors is in the magnitude of 10^{12} cm·HZ$^{1/2}$/W^3. Thus, the D^* of our devices are comparable to those from Si-based photodetectors. The good noise performance shows its feasibility for use in low power or low noise UV detection applications.

Figure 5(a) shows the variation of the photocurrent with the power density of the 375 nm laser. The photocurrents increase significantly under illumination: by varying the power density from 1.06 to 42.36 mW/cm^2, the currents

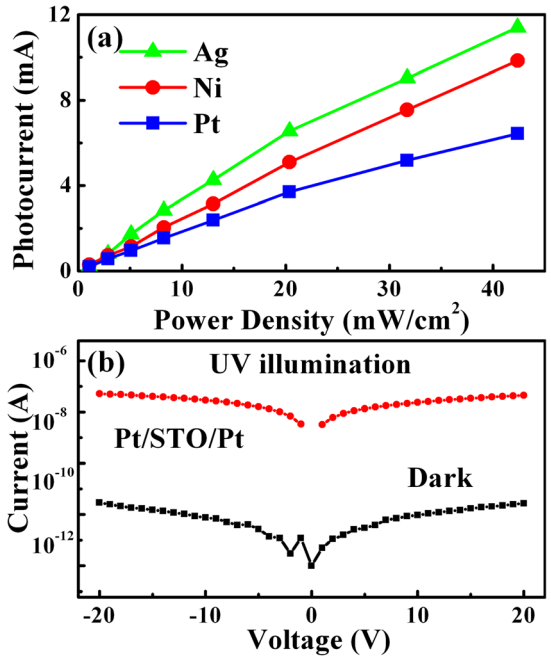

FIG. 5. (a) Variation of photocurrent of the detectors as a function of power density of a 375 nm laser at 10 V bias. (b) A contrast between photocurrent and dark current of the Pt/STO/Pt detector. The photocurrent was measured under the illumination of a 375 nm laser with a power density of 13.02 mW/cm^2.

increase orders of magnitude. It can be seen from Figure 5(a) that the relationship between the photocurrent and the power density is linearity. Figure 5(b) shows a contrast of the photocurrent and dark current of the Pt/STO/Pt detector at 10 V bias. We also found that Ag/STO/Ag and Ni(Au)/STO/Ni(Au) detectors have similar characterization (not shown here). Under the illumination of the 375 nm laser (power density is 13.02 mW/cm^2), the photocurrent increases four orders of magnitude, which demonstrates that the detectors have a good responsivity to UV light.

In addition, the time response characteristic of the devices is measured and shown in Figure 6. The third harmonic of an actively passively mode-locked Nd: YAG laser, operating at a wavelength of 355 nm with 15 ps duration and a 1.5 GHZ digital oscilloscope were used. The sampling resistance is 0.5 Ω. The rise time of the three detectors is 360.9, 301.5, and 394.4 ps, respectively, and the full width at the half-maximum is 576.5, 537.2, and 966.9 ps, respectively. The results indicate that these detectors can be used in ultrafast detection.

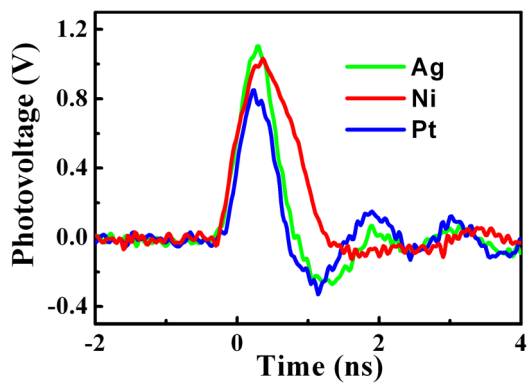

FIG. 6. Typical time response of the detectors under the irradiation of a 355 nm pulsed laser with 15 ps duration.

IV. CONCLUSION

In summary, the electrode-dependent effects of the MSM photodetectors using different types of metals with different work functions were investigated. Low dark current and high detectivity UV photodetectors were demonstrated based on STO single crystals. STO crystals could be taken as slightly acceptor-doped materials, therefore larger Schottky barrier height by using lower work function metal as electrode can be formed. As a result, the Ag/STO/Ag detector has the lowest dark current and the highest responsivity. All the detectors with different metal electrodes exhibit dark currents of 10^{-11} orders of magnitude. The calculated NEP values for the MSM photodetectors with Ag, Ni, and Pt electrodes are 7.09×10^{-15}, 7.50×10^{-15}, and 2.28×10^{-14} W/HZ$^{1/2}$, respectively, which show that the detectors have good noise performance and can be used in high noise environment. In addition, the most important figure of detectors D* are 4.11×10^{12}, 3.88×10^{12}, and 1.27×10^{12} cm·HZ$^{1/2}$/W, respectively, which is comparable to those from Si-based photodetectors. The results show that the MSM photodetectors with Ag, Ni, and Pt electrodes not only economize the material cost but also optimize the performance of the UV photodetector.

ACKNOWLEDGMENTS

This work was supported by the National Basic Research Program of China (Nos. 2012CB921403 and 2013CB328706) and the National Natural Science Foundation of China (Nos. 10825418 and 11134012).

[1]A. H. C. Pernot, A. Hirano, M. Iwaya,T. Detchprohm, H. Amano and I. Akasaki, Jpn. J. Appl. Phys., Part 2 **38**, L487 (1999).
[2]C. J. Collins, T. Li, A. L. Beck, R. D. Dupuis, J. C. Campbell, J. C. Carrano, M. J. Schurman, and I. A. Ferguson, Appl. Phys. Lett. **75**, 2138 (1999).
[3]X. Gong, M. Tong, Y. Xia, W. Cai, J. S. Moon, Y. Cao, G. Yu, C. L. Shieh, B. Nilsson, and A. J. Heeger, Science **325**, 1665 (2009).
[4]R. McClintock, K. Mayes, A. Yasan, D. Shiell, P. Kung, and M. Razeghi, Appl. Phys. Lett. **86**, 011117 (2005).
[5]M. Razeghi and A. Rogalski, J. Appl. Phys. **79**, 7433 (1996).
[6]C. Soci, A. Zhang, B. Xiang, S. A. Dayeh, D. P. R. Aplin, J. Park, X. Y. Bao, Y. H. Lo, and D. Wang, Nano Lett. **7**, 1003 (2007).
[7]D. Walker, A. Saxler, P. Kung, X. Zhang, M. Hamilton, J. Diaz, and M. Razeghi, Appl. Phys. Lett. **72**, 3303 (1998).
[8]A. Sciuto, F. Roccaforte, S. D. Franco, V. Raineri, and G. Bonanno, Appl. Phys. Lett. **89**, 081111 (2006).
[9]E. Assmann, P. Blaha, R. Laskowski, K. Held, S. Okamoto, and G. Sangiovanni, Phys. Rev. Lett. **110**, 078701 (2013).
[10]T. Yajima, Y. Hikita, and H. Y. Hwang, Nature Mater. **10**, 198 (2011).
[11]K. Zhao, K.-J. Jin, Y. Huang, S. Zhao, H. Lu, M. He, Z. Chen, Y. Zhou, and G. Yang, Appl. Phys. Lett. **89**, 173507 (2006).
[12]J. Xing, K. Zhao, H. B. Lu, X. Wang, G. Z. Liu, K. J. Jin, M. He, C. C. Wang, and G. Z. Yang, Opt. Lett. **32**, 2526 (2007).
[13]J. Xing, E. Guo, K.-J. Jin, H. Lu, J. Wen, and G. Yang, Opt. Lett. **34**, 1675 (2009).
[14]E.-J. Guo, J. Xing, H.-B. Lu, K.-J. Jin, J. Wen, and G.-Z. Yang, J. Phys. D: Appl. Phys. **43**, 015402 (2010).
[15]E.-J. Guo, J. Xing, K.-J. Jin, H.-B. Lu, J. Wen, and G.-Z. Yang, J. Appl. Phys. **106**, 023114 (2009).

[16]L. Wang, K.-J. Jin, J. Xing, C. Ge, H.-B. Lu, W.-J. Zhou, and G.-Z. Yang, Appl. Opt. **52**, 3473 (2013).
[17]M. Copel, P. R. Duncombe, D. A. Neumayer, T. M. Shaw, and R. M. Tromp, Appl. Phys. Lett. **70**, 3227 (1997).
[18]R. Schafranek, S. Payan, M. Maglione, and A. Klein, Phys. Rev. B **77**, 195310 (2008).
[19]G. W. Dietz, W. Antpohler, M. Klee, and R. Waser, J. Appl. Phys. **78**, 6113 (1995).
[20]C. Park, Y. Seo, J. Jung, and D. W. Kim, J. Appl. Phys. **103**, 054106 (2008).
[21]M. Mrovec, J. M. Albina, B. Meyer, and C. Elsasser, Phys. Rev. B **79**, 245121 (2009).
[22]J. Robertson and C. W. Chen, Appl. Phys. Lett. **74**, 1168 (1999).
[23]V. E. Henrich, G. Dresselhaus, and H. J. Zeiger, Phys. Rev. B **17**, 4908 (1978).
[24]O. Auciello, *Sience and Technology of Electroceramic Thin Films* (Kluwer Academic Publishers, 1995).
[25]M. H. Francombe and J. D. Adam, *Frontiers of Thin Film Technology* (Academic Press, 2000).
[26]D. Li, X. Sun, H. Song, Z. Li, H. Jiang, Y. Chen, G. Miao, and B. Shen, Appl. Phys. Lett. **99**, 261102 (2011).
[27]S. M. Sze and K. K. Ng, *Physics of Semiconductor Devices*, 3 ed. (Wiley, New York, 2007).
[28]K. W. Liu, J. Y. Zhang, J. G. Ma, D. Y. Jiang, Y. M. Lu, B. Yao, B. H. Li, D. X. Zhao, Z. Z. Zhang, and D. Z. Shen, J. Phys. D: Appl. Phys. **40**, 2765 (2007).
[29]Y. Zhang, S.-C. Shen, H. J. Kim, S. Choi, J.-H. Ryou, R. D. Dupuis, and B. Narayan, Appl. Phys. Lett. **94**, 221109 (2009).